

Synthesis of CdS nanowire networks and their optical and electrical properties

To cite this article: R M Ma *et al* 2007 *Nanotechnology* **18** 205605

View the [article online](#) for updates and enhancements.

You may also like

- [Surface effects on the buckling of nanowire networks](#)
Jin Zhang
- [Transparent, highly flexible, all nanowire network germanium photodetectors](#)
Burcu Aksoy, Sahin Coskun, Seyda Kucukyildiz *et al.*
- [Core/shell copper nanowire networks for transparent thin film heaters](#)
Dogancan Tigan, Sevim Polat Genlik, Bilge Imer *et al.*



ECS The Electrochemical Society
Advancing solid state & electrochemical science & technology

ECS UNITED

247th ECS Meeting
Montréal, Canada
May 18-22, 2025
Palais des Congrès de Montréal

Showcase your science!

Abstracts due December 6th

Synthesis of CdS nanowire networks and their optical and electrical properties

R M Ma¹, X L Wei², L Dai^{1,3}, H B Huo¹ and G G Qin¹

¹ School of Physics and State Key Lab for Mesoscopic Physics, Peking University, Beijing 100871, People's Republic of China

² Key Laboratory for the Physics and Chemistry of Nanodevices and Department of Electronics, Peking University, Beijing 100871, People's Republic of China

E-mail: lundai@pku.edu.cn.

Received 20 January 2007, in final form 25 March 2007

Published 23 April 2007

Online at stacks.iop.org/Nano/18/205605

Abstract

High quality single-crystal CdS nanowire (NW) networks have been synthesized on Si(111) substrates via the chemical vapour deposition method. X-ray diffraction and selected area electron diffraction show that the NWs in the networks grow along the $\langle 11\bar{2}0 \rangle$ directions and their (0001) crystal planes are parallel to the Si(111) substrates. Room-temperature photoluminescence (PL) spectra of single CdS NWs in the networks are dominated by a near-band-edge emission and free from deep-level defect emissions. The PLs resulting from free-exciton and bound-exciton recombinations are detected at 77 K. The results of the electrical transport measurement on the CdS NW networks show that the current can flow through different NWs via the cross-junctions. The resistivity, electron concentration and electron mobility of single NWs in the networks are estimated by fitting the I - V curves measured on single NWs with the metal-semiconductor-metal model suggested by Zhang *et al* (2006 *Appl. Phys. Lett.* **88** 073102; 2007 *Adv. Funct. Mater.* at press).

1. Introduction

CdS, with a direct bandgap of 2.4 eV at room temperature, is one of the most important group II-VI semiconductors and has been widely used in making optoelectronic and electronic devices. Recently, a variety of one-dimensional (1D) CdS nanostructures, such as nanowires (NWs) [1], nanotubes [2] and nanobelts (NBs) [3] have been synthesized. Various 1D CdS nanodevices, such as photoconductive optical switches [4, 5], electro-optic modulators [6], field-effect transistors (FETs) [7-11], light emitting diodes (LEDs) [8, 12, 13] and electrically driven laser have been fabricated successfully [14].

The application of 1D nanostructures which can serve as building blocks for nanodevices depends not only on their physical/chemical properties, but also on their special orientation and arrangement. Oriented and aligned 1D nanostructures have shown their excellent performance in lasers [15], sensors [16], LEDs [17-19], address decoders [20], field-emission devices [21], FETs [22, 23], nano-generators [24], etc. To date,

most reported NW arrays were grown perpendicularly from the substrate [15, 17-19, 21-25]. NWs which are highly oriented and well aligned in a plane parallel to the substrate have the advantage in assembling functional nanodevices [20, 26-28]. In this paper we report, for the first time, the synthesis of CdS NW networks on Si(111) substrates via the chemical vapour deposition (CVD) method. The single-crystal wurtzite CdS NWs grow along the $\langle 11\bar{2}0 \rangle$ directions and form a network in a plane parallel to the Si(111) substrate. An *in situ* indium (In) doping method has been used to enhance the conductivity of the NWs in the networks [8]. The electrical transport measurement results show that the CdS NWs in the networks have high electrical quality, and the current can flow through different NWs via the cross-junctions.

2. Experiment

The CdS NW networks on Si(111) substrates were synthesized via the CVD method. CdS (99.995%) powders were used as the source and pieces of Si(111) wafer covered with 10 nm thick thermally evaporated Au catalyst were used as the substrates. Before Au evaporation, the Si(111) substrates were cleaned by

³ Author to whom any correspondence should be addressed.

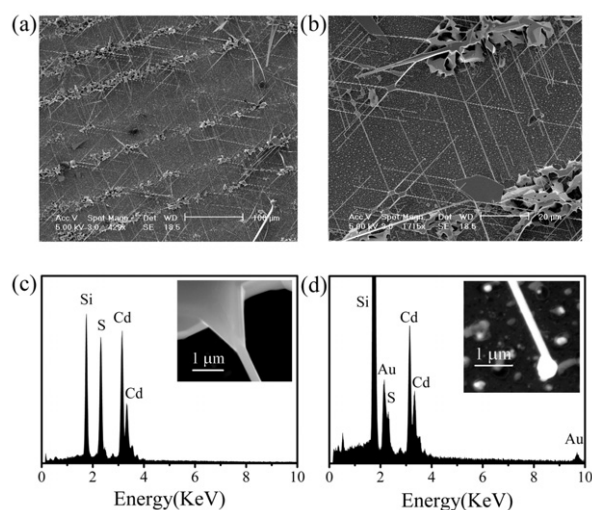


Figure 1. (a), (b) SEM images of CdS NW networks on Si(111) substrate under different magnification. (c), (d) The EDX spectra taken from the CdS NW and the nanoparticle at the end of the NW, respectively. The insets of (c), (d) show the SEM images of the 'root' part of a CdS NW and the nanoparticle at the end of the NW, respectively.

a standard treatment in a piranha solution ($\text{H}_2\text{O}_2:\text{H}_2\text{SO}_4 = 1:3$), followed by a 10 s rinse in a HF buffer solution. Prior to heating, the quartz tube inside the tube furnace was cleaned with high-purity argon (Ar) for 90 min. Then under a constant flow of Ar (20 sccm), the furnace was rapidly heated to 870 °C. A quartz boat loaded with CdS powders and Si(111) substrates was inserted into the quartz tube, with the CdS at the upstream of the Ar gas. The distance between the CdS powders and Si(111) substrates was about 15 cm. The synthesis duration was about 1 h. The In-doped CdS NW networks, where In acts as shallow donor [8], were synthesized with a similar process, except that, during the synthesis, a small grain of In was added on the quartz boat 20 cm away from the CdS powders at the upstream of Ar gas. The synthesized products were characterized using an x-ray powder diffractometer (XRD) (Rigaku Dmax-2000), a field-emission environmental scanning electron microscope (SEM) (Quanta 200F) equipped with an energy-dispersive x-ray spectroscope (EDX) and a high-resolution transmission electron microscope (HRTEM) (Tecnai F30). The photoluminescence (PL) measurements on single CdS NWs in the networks were done with a microzone confocal Raman spectrometer (HORIBA Jobin Yvon, LabRam HR800) equipped with a colour charge-coupled device (CCD) camera and a cooling/heating stage (Linkam THMS 600). The 325 nm line of a He–Cd laser (Kimmon IK3301R-G) was used as the excitation source. The room-temperature electrical transport measurements were done using a nanoprobe system (Kleindiek MM3A) installed in a SEM (FEI XL 30F) [29]. The chemically etched tungsten tips were used as the nanoprobes. The nanoprobe system was connected to a semiconductor characterization system (Keithley 4200).

3. Results and discussion

The SEM images, XRD, EDX, selected area electron diffraction (SAED) data and the PL spectra of unintentionally

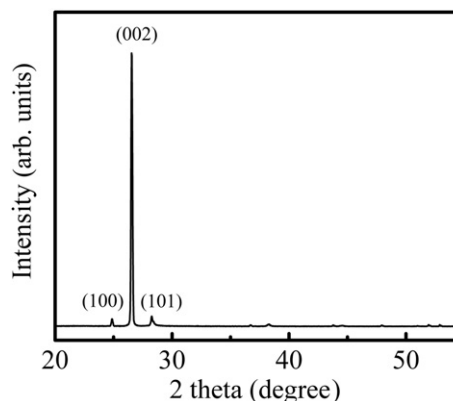


Figure 2. X-ray diffraction (XRD) pattern of the CdS NW networks.

doped CdS NW networks are similar to those of In doped ones, respectively. Figures 1(a) and (b) show typical SEM images of the CdS NW networks under different magnification. We can see that the NWs have smooth surfaces and uniform diameters, grow from the side surfaces of some micro-scale structures along six symmetric directions, and form the networks. Usually, the CdS NWs are some tens of microns in length and 200 nm in diameter. The space distances between the NWs in the networks are about several microns. The inset of figure 1(c) shows a magnified image of the 'root' part of a NW, where the NW grows epitaxially from a micro-scale structure. The EDX spectra of the microstructure and the NW are similar, indicating that they are composed of only Cd and S. A typical one is shown in figure 1(c). The inset of figure 1(d) shows a magnified image at the other end of the NW depicted. We can see clearly that the NW terminates with a nanoparticle. The EDX spectrum of the nanoparticle (shown in figure 1(d)) indicates that it is composed of Au, Cd and S. Figure 2 shows a typical x-ray diffraction (XRD) pattern of the sample. We can see a strong dominated diffraction peak, which can be indexed as (0002) of the wurtzite CdS (JCPDS 80-0001). This indicates that the (0001) crystal planes of the CdS microstructures and NW networks are parallel to Si(111) substrate. The several weak diffraction peaks may come from some randomly oriented CdS NWs.

We have also investigated the crystalline characteristic of the NWs near the cross-junctions, where the NWs growing along different directions cross each other. Figure 3 shows a TEM image of a cross-junction. Most of the NWs were broken during the ultrasonic process in making the TEM sample. The insets of figure 3 are the SAED patterns recorded along the [0001] zone axis at the circled areas of two different NW branches of the cross-junction. The SAED results demonstrate that the NWs are single-crystal wurtzite CdS, the growth directions are $(11\bar{2}0)$ and the (0001) crystal planes of the CdS NWs are parallel to the Si(111) substrate, consistent with the XRD result. It is worth pointing out that the CdS NW networks cannot be synthesized without using either Si(111) substrates or Au catalyst in our experimental conditions. In other words, both Si(111) substrates and Au catalyst are crucial for the formation of CdS NW networks.

We suggest that there are two processes in the synthesis of CdS NW networks. Firstly, single-crystal CdS microstructures

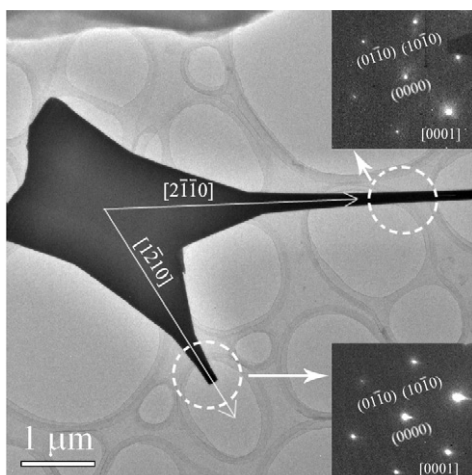


Figure 3. A TEM image of a cross-junction. The insets are the SAED patterns taken from the two NW branches at the circled areas.

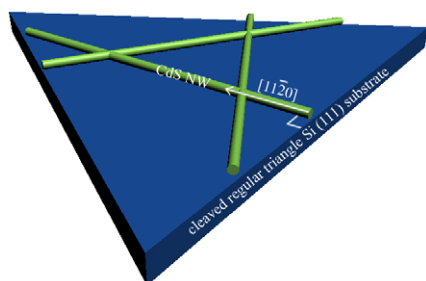


Figure 4. Schematic illustration of single-crystal wurtzite CdS NW networks grown on cleaved regular triangle Si(111) substrate.

grow heteroepitaxially from the surface of the Si(111) substrate. The surface of Si(111) wafer presents a hexagonal plane of tetrahedrally bonded Si atoms. There is only 7% mismatch between the atoms in the Si(111) plane and the (0001) plane of hexagonal wurtzite CdS, which allows for the heteroepitaxial growth of CdS on Si(111) [30, 31]. Secondly, the CdS NWs grow from the $\{11\bar{2}0\}$ planes of the CdS microstructures via a homoepitaxial process and form the networks. The 10 nm Au thin film will change into Au nanoclusters and/or nanoparticles when the substrate is heated in the growth process. These Au nanostructures will catalyze both CdS microstructures and CdS NWs to grow on the Si substrate in our case. The growths of both CdS microstructures and CdS NWs are based on the well-known Au-catalyzed vapour-liquid-solid (VLS) process [32]. We have also used the cleaved regular triangle Si(111) wafers as the substrates to synthesize the CdS nanowire networks. The six symmetric $\langle 11\bar{2}0 \rangle$ growth directions of the synthesized CdS nanowires are perpendicular to the three sides of the regular triangle Si(111) substrate, respectively, which is direct evidence that the $\langle 11\bar{2}0 \rangle$ growth directions of single-crystal wurtzite CdS relate to the lattice of the Si(111) surface and such a relationship is in accordance with the theoretical expectancy of epitaxial growth. Figure 4 shows the schematic illustration of such a relationship.

Figure 5 shows the normalized room-temperature and 77 K PL spectra of a single CdS NW in the networks. The room-temperature PL spectrum is dominated by an emission

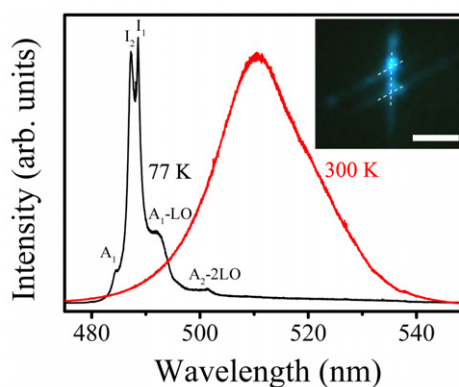


Figure 5. PL spectra of a single CdS NW in the networks measured at 300 and 77 K. The inset is the PL image of several crossed CdS NWs in the networks recorded by the colour CCD camera at 77 K. The positions of the involved CdS NWs are represented with dashed lines. The scale bar is 1 μm .

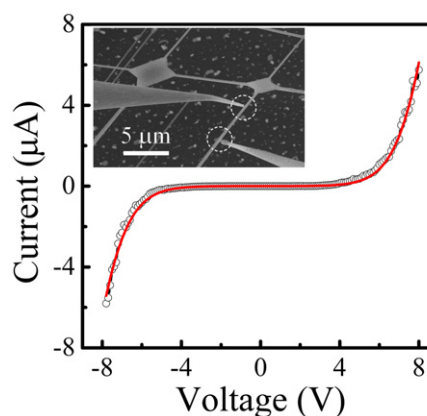


Figure 6. The I - V curve of a single CdS NW in the networks. The scattered hollow circles are experimental data and the solid line is a fitted I - V curve. Inset: SEM image of the NW contacted by two tungsten probes. The contact positions of the nanoprobe with the NW are circled by the dashed lines.

peaked at 510 nm, which is the near-band-edge emission from CdS. No deep-level defect emissions are observed. With the temperature falling, the near-band-edge PL intensity increases, and its wavelength exhibits a blueshift along with the broadening of the bandgap. At 77 K, several excitonic emission peaks are resolved. The two intense sharp peaks at 2.545 and 2.538 eV can be assigned to I_2 and I_1 , respectively. The I_2 and I_1 are the radiative recombination of the excitons bounded to neutral donors and neutral acceptors, respectively [33]. The weak peak at 2.559 eV can be assigned to free-exciton recombination (A_1) [30]. Two phonon replicas of A_1 , labelled as A_1 -LO and A_1 -2LO, are also observed. The observed free-exciton and bound-exciton emission peaks show that the synthesized NWs are with very high crystalline and optical quality. The inset of figure 5 shows a 77 K PL image of several crossed CdS NWs. Blue light can be seen clearly emitting from the NWs. The actual positions of the involved CdS NWs are represented with dashed lines.

The electrical transport properties of In-doped CdS NW networks were studied. First, we moved the two nanoprobe

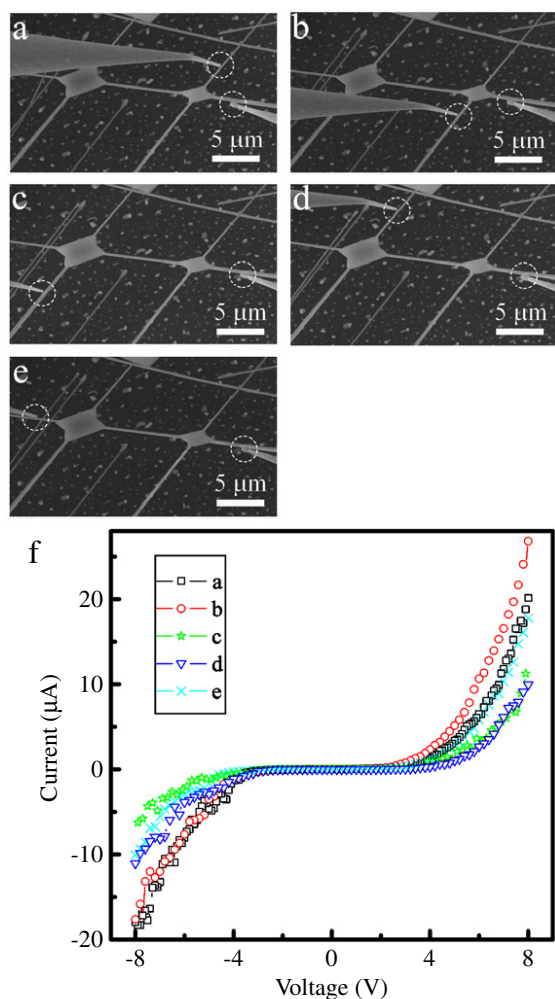


Figure 7. (a)–(e) SEM images of the NW networks contacted by two tungsten probes. There are altogether six NW branches and two cross-junctions involved in this measurement. The contact positions of the nanoprobe with the NWs are circled by dashed lines. (f) Representative two-terminal I – V curves corresponding to (a)–(e) experimental set-ups.

(This figure is in colour only in the electronic version)

into contact with a single NW. The corresponding SEM image and I – V curve (scattered hollow circles) are shown in figure 6. The I – V curve show an almost symmetric non-ohmic contact behaviour resulting from the back-to-back Schottky contacts formed between the tungsten nanoprobe and the CdS NW. Zhang *et al* have suggested a metal–semiconductor–metal (M–S–M) model to analyse quantitatively the I – V characteristics of such a M–S–M system [34, 35]. Using this model, we can reproduce the observed I – V characteristics using a few fitting variables, and estimate the intrinsic parameters of the NW. The fitted values of resistivity, electron concentration and electron mobility of the CdS NW are $(0.14 \pm 0.04) \Omega \text{ cm}$, $(2.7 \pm 0.2) \times 10^{17} \text{ cm}^{-3}$ and $(170 \pm 50) \text{ cm}^2 \text{ V}^{-1} \text{ s}^{-1}$, respectively. These values are in accordance with the values we obtained previously by measuring In-doped CdS single nanobelt FETs [8, 11]. Later, we fixed one nanoprobe into contact with one NW branch, and moved the other one into contact with other NW branches in sequence. The SEM images

of the NW networks contacted by two tungsten probes are shown in figures 7(a)–(e). Figure 7(f) shows the corresponding I – V curves. All the I – V curves show an almost symmetric non-ohmic contact behaviour similar to that measured on single NW. These results indicate that the NWs in the networks have high electrical quality, and the current can flow through different NWs via the cross-junctions.

4. Conclusion

High quality single-crystal CdS NW networks have been synthesized on Si(111) substrates via the simple CVD method. CdS NWs are grown homoepitaxially from the $\{11\bar{2}0\}$ surfaces of CdS microstructures and form networks in a plane parallel to the Si(111) substrates. The (0001) crystal planes of both CdS microstructures and NW networks are parallel to Si(111) substrates. The room-temperature PL spectra of single CdS NW in the networks are dominated by near-band-edge emission and free from deep-level defect emissions. Free-exciton and bound-exciton emissions can be observed in 77 K PL spectra of single CdS NW. The electrical transport measurement results on the CdS NW networks show that the current can flow through different NWs via the cross-junctions. The intrinsic parameters of the single CdS NWs are estimated by using an M–S–M model. Our results show that the CdS NW networks have high crystalline, optical and electrical qualities. Highly oriented CdS NW networks have the potential for building dense nano-optoelectronic devices.

Acknowledgments

This work was supported by the National Natural Science Foundation of China under grant nos. 60576037, 10574008 and 60476023, and National Basic Research Program of China (No. 2006CB921607).

References

- [1] Xu D S, Xu Y J, Chen D P, Guo G L, Gui L L and Tang Y Q 2000 *Adv. Mater.* **12** 520
- [2] Xiong Y J, Xie Y, Yang J, Zhang R, Wu C Z and Du G J 2002 *J. Mater. Chem.* **12** 3712
- [3] Dong L F, Jiao J, Coulter M and Love L 2003 *Chem. Phys. Lett.* **376** 653
- [4] Gao T, Li Q H and Wang T H 2005 *Appl. Phys. Lett.* **86** 173105
- [5] Jie J S, Zhang W J, Jiang Y, Meng X M, Li Y Q and Li S T 2006 *Nano Lett.* **6** 1887
- [6] Gretyak A B, Barrelet C J, Li Y and Lieber C M 2005 *Appl. Phys. Lett.* **87** 151103
- [7] Duan X, Niu C, Sahi V, Chen J, Parce J W, Empedocles S and Goldman J L 2003 *Nature* **425** 274
- [8] Ma R M, Dai L, Huo H B, Yang W Q, Qin G G, Tan P H, Huang C H and Zhen J 2006 *Appl. Phys. Lett.* **89** 203120
- [9] Jie J S, Zhang W J, Jiang Y and Lee S T 2006 *Appl. Phys. Lett.* **89** 223117
- [10] Ma R M, Dai L and Qin G G 2007 *Appl. Phys. Lett.* **90** 093109
- [11] Ma R M, Dai L and Qin G G 2007 *Nano Lett.* **7** 868
- [12] Huang Y, Duan X and Lieber C M 2005 *Small* **1** 142
- [13] Hayden O, Gretyak A B and Bell D C 2005 *Adv. Mater.* **17** 701
- [14] Duan X, Huang Y, Agarwal R and Lieber C M 2003 *Nature* **421** 241
- [15] Huang M H, Mao S, Feick H, Yan H Q, Wu Y Y, Kind H, Weber E, Russo R and Yang P D 2001 *Science* **292** 1897
- [16] Ponzoni A, Comini E, Sberveglieri G, Zhou J, Deng S Z, Xu N S, Ding Y and Wang Z L 2006 *Appl. Phys. Lett.* **88** 203101

- [17] Park W I and Yi G C 2004 *Adv. Mater.* **16** 87
- [18] Konenkamp R, Word R C and Schlegel C 2004 *Appl. Phys. Lett.* **85** 6004
- [19] Konenkamp R, Word R C and Godinez M 2005 *Nano Lett.* **5** 2005
- [20] Zhong Z H, Wang D L, Cui Y, Bockrath M W and Lieber C M 2003 *Science* **302** 1377
- [21] Li Y F, Hsu Y J, Lu S Y and Kung S C 2006 *Chem. Commun.* **22** 2391
- [22] Ng H T, Han J, Yamada T, Nguyen P, Chen Y P and Meyyappan M 2004 *Nano Lett.* **4** 1247
- [23] Goldberger J, Hochbaum A I, Fan R and Yang P D 2006 *Nano Lett.* **6** 973
- [24] Wang Z L and Song J H 2006 *Science* **312** 242
- [25] Yang W Q, Huo H B, Dai L, Ma R M, Liu S F, Ran G Z, Shen B, Lin C L and Qin G G 2006 *Nanotechnology* **17** 4868
- [26] Whang D, Jin S and Lieber C M 2003 *Nano Lett.* **3** 951
- [27] Whang D, Jin S, Wu Y and Lieber C M 2003 *Nano Lett.* **3** 1255
- [28] Huang Y, Duan X F, Wei Q Q and Lieber C M 2001 *Science* **291** 630
- [29] Peng L M, Chen Q, Liang X L, Gao S, Wang J Y, Kleindiek S and Tai S W 2004 *Micron* **35** 495
- [30] Berry A K, Amirtharaj P M, Du J-T, Boone J L and Martin D D 1992 *Thin Solid Films* **219** 153
- [31] Seto S 2005 *Japan. J. Appl. Phys.* **44** 5913
- [32] Gudiksen M S, Wang J F and Lieber C M 2001 *J. Phys. Chem. B* **105** 4062
- [33] Wang C, Lp K M, Hark S K and Li Q 2005 *J. Appl. Phys.* **97** 054303
- [34] Zhang Z Y, Jin C H, Liang X L, Chen Q and Peng L-M 2006 *Appl. Phys. Lett.* **88** 073102
- [35] Zhang Z Y, Yao K, Liu Y, Jin C H, Liang X L, Chen Q and Peng L-M 2007 *Adv. Funct. Mater.* at press